Naval Research Laboratory
Washington, DC 20375-5320

NRL/6170/MR—2023/3

Deactivation of End-of-Life Batteries

GORDON H. WALLER

RACHEL CARTER

COREY T. LOVE

Surface Chemistry Branch
Chemistry Division

September 13, 2023

REPORT DOCUMENTATION PAGE

Form Approved
OMB No. 0704-0188

1. REPORT DATE *(DD-MM-YYYY)*	**2. REPORT TYPE**	**3. DATES COVERED** *(From - To)*
13-09-2023	NRL Memorandum Report	10/1/22 – 8/16/23

4. TITLE AND SUBTITLE

Deactivation of End-of-Life Batteries

5a. CONTRACT NUMBER

5b. GRANT NUMBER

5c. PROGRAM ELEMENT NUMBER

6. AUTHOR(S)

Gordon H. Waller, Rachel Carter, and Corey T. Love

5d. PROJECT NUMBER

5e. TASK NUMBER

5f. WORK UNIT NUMBER
1A49

7. PERFORMING ORGANIZATION NAME(S) AND ADDRESS(ES)

Naval Research Laboratory
4555 Overlook Avenue, SW
Washington, DC 20375-5320

8. PERFORMING ORGANIZATION REPORT NUMBER

NRL/6170/MR--2023/3

9. SPONSORING / MONITORING AGENCY NAME(S) AND ADDRESS(ES)

Mr. Joshua Davis
Department of Transportation Pipeline and Hazardous Materials Safety Administration
1200 New Jersey Avenue, S.E.
Washington, DC 20590

10. SPONSOR / MONITOR'S ACRONYM(S)

DOT PHMSA

11. SPONSOR / MONITOR'S REPORT NUMBER(S)

12. DISTRIBUTION / AVAILABILITY STATEMENT

DISTRIBUTION STATEMENT A: Approved for public release; distribution is unlimited.

13. SUPPLEMENTARY NOTES

14. ABSTRACT

Batteries can contain significant amounts of energy at the end of life. Improper handling during transportation or disposal of end-of-life batteries can lead to fires and chemical exposures. This report explores methods to deactivate end-of-life batteries by removing all residual energy, with an emphasis on energy-dense lithium-ion cells. A review of industrial and academic deactivation methods is provided, along with an experimental evaluation of salt-water immersion as a deactivation method conducted at the Naval Research Laboratory.

15. SUBJECT TERMS

Battery Battery deactivation

16. SECURITY CLASSIFICATION OF:			**17. LIMITATION OF ABSTRACT**	**18. NUMBER OF PAGES**	**19a. NAME OF RESPONSIBLE PERSON**
					Gordon H. Waller
a. REPORT	**b. ABSTRACT**	**c. THIS PAGE**	U	41	**19b. TELEPHONE NUMBER** *(include area code)*
U	U	U			(202) 404-3355

This page intentionally left blank.

CONTENTS

1. INTRODUCTION 1
2. OVERVIEW OF BATTERY HAZARDS 4
3. DEACTIVATION METHODS 6
4. EXPERIMENTAL EVALUATION OF SALTWATER IMMERSION 10
   4.1 ELECTROLYSIS OF SALTWATER SOLUTIONS 12
   4.2 CORROSION OF COMMON CELL MATERIALS IN SALTWATER 17
   4.3 IMMERSION OF COMMERCIAL LITHIUM-ION CELLS IN SALTWATER 27
5. CONCLUSIONS AND RECOMMENDATIONS 33
6. REFERENCES 34

FIGURES

Figure 1 Saltwater solution conductivity as a function of concentration (left) and molarity (right)..... 10
Figure 2 Saltwater solution pH as a function of concentration (left) and molarity (right)..... 11
Figure 3 Solution conductivity vs. solution temperature for $(NH_4)H_2PO_4$ solutions. 11
Figure 4 Schematic (left) and photograph (right) of three-electrode electrochemical cell. 12
Figure 5 Current vs. Voltage (I vs. V) plot produced by a cyclic voltammogram of 3.5 wt% NaCl, 5.8 wt% $(NH_4)HCO_3$, and 11 wt% $(NH_4)H_2PO_4$ saltwater solutions using three-electrode test cell. 14
Figure 6 Current vs. Voltage (I vs. V) plot produced by a cyclic voltammogram of 5 wt%, 11 wt%, and 20 wt% $(NH_4)H_2PO_4$ solutions using three-electrode test cell. 15
Figure 7 Current vs. time response for $(NH_4)H_2PO_4$ solutions subjected to +4V in a two-electrode test cell. 16
Figure 8 Average current for +4V two-electrode electrolysis of $(NH_4)H_2PO_4$ solutions. 16
Figure 9 Current vs. Voltage (I vs. V) plot produced by a cyclic voltammogram of 5 wt%, 11 wt%, and 20 wt% $(NH_4)H_2PO_4$ solutions using two-electrode cell with aluminum electrodes. 18
Figure 10 Current vs. Voltage (I vs. V) plot produced by a cyclic voltammogram of 5 wt%, 11 wt%, and 20 wt% $(NH_4)H_2PO_4$ solutions using two-electrode cell with copper electrodes. 19
Figure 11 Current vs. Voltage (I vs. V) plot produced by a cyclic voltammogram of 5 wt%, 11 wt%, and 20 wt% $(NH_4)H_2PO_4$ solutions using two-electrode cell with nickel electrodes. 20
Figure 12 Current vs. Voltage (I vs. V) plot produced by a cyclic voltammogram of 5 wt%, 11 wt%, and 20 wt% $(NH_4)H_2PO_4$ solutions using two-electrode cell with steel electrodes..... 20
Figure 13 Current (A) vs. test time (hours) plot produced during potentiostatic electrolysis experiment in 11 wt%$(NH_4)H_2PO_4$ solutions..... 21
Figure 14 Current (A) vs. test time (hours) plot produced during potentiostatic electrolysis experiment in 5.8 wt% $(NH_4)HCO_3$ solutions. 22
Figure 15 Current (A) vs. test time (hours) plot produced during potentiostatic electrolysis experiment in 3.5 wt% NaCl solutions. 22
Figure 16 Positive electrode mass loss during a 10-hour electrolysis experiment as a function of applied potential and electrode material in 11 wt%$(NH_4)H_2PO_4$ solutions. 23
Figure 17 Positive electrode mass loss during a 10-hour electrolysis experiment as a function of applied potential and electrode material in 5.8 wt% $(NH_4)HCO_3$ solutions. 24
Figure 18 Positive electrode mass loss during a 10-hour electrolysis experiment as a function of applied potential and electrode material in 3.5 wt% NaCl solutions. 24
Figure 19 Energy dissipated during a 10-hour electrolysis experiment as a function of applied potential and electrode material in 11 wt% $(NH_4)H_2PO_4$ solutions. 25
Figure 20 Energy dissipated during a 10-hour electrolysis experiment as a function of applied potential and electrode material in 5.8 wt% $(NH_3)HCO_3$. 26
Figure 21 Energy dissipated during a 10-hour electrolysis experiment as a function of applied potential and electrode material in 3.5 wt% NaCl. 26
Figure 22 Voltages of 18650 lithium-ion cells immersed in iso-conductive saltwater solutions. 27
Figure 23 Photographs of saltwater solution, positive terminal, and negative terminal of 18650 lithium-ion cells after 24 hours of immersion..... 29
Figure 24 Photographs of saltwater solution, positive terminal, and negative terminal of 18650 lithium-ion cells after 96 hours of immersion..... 30
Figure 25 Photographs of 18650 lithium-ion cell anode (A) and cathode (C) after electrical discharge to 0V or 96 hours in saltwater solutions..... 31
Figure 26 Voltage, pressure, and temperature response of 18650 lithium-ion cells subjected to external heating inside of a pressure vessel after 24 hours in saltwater solutions. 31
Figure 27 Voltage, pressure, and temperature response of 18650 lithium-ion cells subjected to external heating inside of a pressure vessel after 72 hours in saltwater solutions. 32

TABLES

Table 1 Comparison of deactivation methods.. 8

This page intentionally left blank.

EXECUTIVE SUMMARY

The following report was prepared by the U.S. Naval Research Laboratory on behalf of the U.S. Department of Transportation Pipeline and Hazardous Materials Safety Agency (DOT PHMSA). The contents of this report include an overview of the hazardous associated with high-energy electrochemical devices (i.e., batteries) presented in Section 2, a review of methods to deactivate batteries at the end of useful life presented in Section 3, and an experimental evaluation of one method identified as a promising low cost and general purpose – saltwater immersion – presented in Section 3.

Lithium-ion batteries and other high-energy electrochemical energy storage devices provide critical power to a variety of applications, however high energy density is directly correlated with the possibility of energetic failures. Deactivation of batteries and the end of life can prevent these energetic failures and enable lower cost, lower hazard transportation of these devices, ideally resulting in an improved rate of recycling. Among the broad categories of deactivation techniques identified (e.g. saltwater immersion, electrical discharge, and mechanical shredding), saltwater immersion was concluded to be the most readily applicable to a wide range of devices.

An experimental evaluation of saltwater immersion found that while saltwater duration did successfully deactivate lithium-ion cells, the deactivation rate was still relatively slow. Small-scale experiments using single, 2.5 Ah, ~ 4V lithium-ion cells immersed in saltwater required greater than 24 hours to achieve an inert state, and in some cases introduced additional hazards due to the release of the battery electrolyte into the saltwater solution. Electrolysis experiments using idealized electrode materials determined that electrolysis current, which is assumed to be the limiting factor for deactivate rate, could be increased by increasing solution concentration and temperature. Generation of hydrogen and corrosion of metal electrodes are major limitations of saltwater immersion as a deactivation approach. In the case of solutioning containing NaCl as the dissolved salt, corrosion led to cell breaching and plausible release of the electrolyte material into the saltwater solution.

More development of deactivation methods, including a careful assessment of the economic, environmental, and safety impacts of these methods, is needed to provide effective options for emergency responders and battery recyclers tasked with handling and transporting end of life batteries.

This page intentionally left blank.

1. INTRODUCTION

Electrochemical energy storage devices, commonly referred to as batteries, are a critical enabling technology for a variety of electrical devices. Lithium-ion batteries (LIB) are the state-of-the-art in rechargeable battery technologies, with energy densities typically ranging from 300-700 Wh/L depending on the exact chemistry and construction. Maximizing battery energy density is desirable for most applications as this translates to increased operational time for the device. However, increasing energy density also increases the severity of battery failures in which the stored energy of the device is rapidly dissipated (1). LIB have been indicated in many high-profile battery failures and recalls, including the 787 Dreamliner, Samsung Galaxy Note 7, and Chevrolet Volt (2) (3). In these incidents and many others, failures were attributed to manufacturing defects internal to cells and the energy content within the battery itself was sufficient to lead to a fire. In some examples of the Chevrolet Volt and other electric vehicles, these fires propagated through the entire battery pack, destroying the vehicle, and damaging nearby property.

Batteries free of manufacturing defects also present hazards when improperly disposed of. A report from the Environmental Protection Agency published in 2021 studied the role of lithium-ion batteries in fires reported at waste management and recycling facilities (4). This report concluded that among 245 fires occurring at these facilities from 2013 through 2020, 89% were "definitely caused by lithium-ion batteries" and the remainder were reported as "likely caused by lithium-ion batteries". Furthermore, the report concludes that the most common type of lithium-ion battery leading to a facility fire was cell phone battery. In 2021, the top selling smartphone was the iPhone 12 and similar variants from Apple, Samsung, and Xiaomi (5). The iPhone 12 has a single-cell lithium-ion battery with a nameplate energy content 10.78 Wh – roughly equivalent to two 9V alkaline batteries used in smoke detectors (6) (7). This comparison highlights the relatively modest amount of energy needed to lead to costly and dangerous fires under the wrong conditions. Such conditions have occurred during transportation of end-of-life batteries in some instances.

Manuscript approved September 12, 2023.

Two recent examples of transportation related battery incidents involved containers illegally loaded with discarded lithium batteries which caught fire. In an example from 2021, a container of discarded batteries enroute to the Port of Virginia caught fire on the highway, “resulting in loss of the cargo, and significant damage to the shipping container” and “the fire burned hot enough to create a hole through the metal container’s structure” (8). In a second example, a shipping container held at the San Pedro Bay port complex waiting to be loaded onto a ship caught fire, resulting in 40 firefighters being called to respond (9). In both examples, the lithium batteries were undeclared or mis-declared.

Due to the possibility of energetic failures during both routine operation and disposal, methods to deactivate end-of-life batteries are needed. Ideally, a deactivation method could be applicable to any type of cell or battery, have acceptable cost, and not create any additional hazards during or after the deactivation process. Some deactivation methods have been reported in academic literature or applied in industrial settings, and these methods will be described in this report. In general, existing deactivation methods are focused on enabling battery recycling for recovery of critical materials. In a white paper from Underwriters Laboratory, the authors point out that the typical recycling process of lead-acid batteries, which involves crushing batteries to release electrolyte and electrodes from battery casing prior to sorting, is incompatible with lithium-ion batteries due to the creation of internal short circuits (10). The UL report also states, “Discharging or neutralizing any stored charge in batteries before opening or shredding them for recycling can improve the safety of subsequent steps but presents its own set of challenges. Discharging batteries individually, as well as the recovery of useful chemical components, can add significant costs to the process.” A 2020 report from the U.S. Energy Storage Association highlights issues facing recycling large format lithium-ion energy storage systems, stating, “The recycling process begins with dismantling electrically discharged batteries. The current diversity of Li-ion battery types, sizes, and chemistries makes this process difficult to automate, so it must largely be done manually.” (11) In emergency situations, options are even more limited. A 2020 report from the National Transportation Safety Board concludes, “Existing methods of deenergizing a battery (such as accessing the terminals manually or flooding the battery pack with a conductive solution) are not within an emergency responder’s scope and typically take an impractically long time.” (2) While emergency situations are not the explicit focus on this report,

considerations of ease of use and time required for complete deactivation are generally applicable to all scenarios in which battery deactivation is required.

2. OVERVIEW OF BATTERY HAZARDS

During failure, lithium-ion batteries present both thermal hazards as well as chemical hazards. "Thermal runaway" results from a cascade of exothermic chemical reactions which are typically reported to begin at temperatures on the order of 100 °C (12) (13). These reactions can be initiated by external heating, for example due to heat released by an adjacent failed cell, or through mechanical abuse (e.g. crush or penetration), electrical abuse (e.g. overcharge or exceeding current limits) or through internal defects causing electrical short-circuits. Heat generated during thermal runaway leads to volatilization and venting of the flammable organic solvent-based electrolyte used in LIB. The severity of thermal runaway in terms of total heat release correlates strongly with state of charge (SOC). It is generally accepted that lithium-ion batteries at 100% SOC are at their most unstable state, and therefore are at greatest risk for thermal runaway and show the most severe response to abuse (14) (15). At sufficiently low SOC, thermal runaway can be avoided in cells subjected to abuse. However, the threshold SOC below which benign abuse response is observed depends on both the battery and the method of abuse. Lee et al. reported that arrays of 12 small LIB cells at 50% or 100% SOC tested under nitrogen atmosphere underwent complete propagation in response to the forced failure of a single cell by external heating (16). Joshi et al. evaluated eight commercial LIB cell types and found that in every case, thermal runaway was not observed for cells at 0% SOC subjected to external heating (17)**.** However, the same report observed that thermal runaway did occur in some cells at as low as 15% SOC, but with higher onset temperatures and lower maximum temperatures. Joshi et al. and Barai et al. reported on the response of LIB subjected to external short circuit as a function of SOC, with Barai reporting fires for cells tested as low as 15% SOC and Joshi only observing energetic failure (thermal runaway and/or high temperatures) for higher states of charge (17) (18)**.** While SOC is a critical factor determining the possibility and severity of cell failure, it is important to recognize that the chemical energy content of a lithium-ion battery exceeds that of the electrical energy content, which is the quantity expressed by the SOC. Even at 0% SOC lithium-ion batteries still contain significant chemical energy, which can contribute to the total heat release of fires. In a report prepared by Exponent Inc. for the National Fire Protection Agency, the total heat energy released by burning small cells was measured by Oxygen Consumption Calorimetry (19). The total heat released by cells at 0% SOC was only 16% less than cells at 100% SOC. Meanwhile, cells at 100% SOC had more than ten times the peak heat release rate, which reflects the intensity of the battery fires. Suppression of LIB fires is also notably more difficult than fires due to packaging or liquid fuels due to the large thermal mass of LIB undergoing thermal runaway (20). Furthermore, thermal runaway in LIB does not require oxygen to initiate or proceed. Fire suppression approaches which remove oxygen from a combustion event (e.g. carbon dioxide or halon fire suppressants) can be effective in responding to electrolyte fires, however heat

generated by thermal runaway can lead to re-ignition of LIB fires after fire suppression is applied. Effective fire suppression of LIB fires requires cooling the batteries, so water is generally recommended.

Chemical hazards of LIB are particularly prominent during battery fires, which have been reported to release several dangerous compounds due to the combustion of the electrolyte. Larrson et al. subjected a variety of LIB cell types to an open flame experiment and reported the release of hydrofluoric acid (HF) and phosphorous oxyfluoride (POF_3) due to the decomposition of the lithium hexafluorophosphate ($LiPF_6$)electrolyte salt (21). HF concentrations ranged from 20-200 mg per watt-hour of nameplate battery energy content and 15-22 mg per watt hour POF_3. The authors also reported an increase in HF generation for burning LIB exposed to a water mist fire mitigation due to a chemical reaction between the $LiPF_6$ and water, however the total quantity of HF was reduced relative to unmitigated fires. Researchers at the Federal Aviation Administration reported that both the volume and composition of gases emitted in response to external heating were functions of SOC (22). For single 18650 cells, the gas volume increased by a nearly a factor of 10 between 10% and 100% SOC. Notable increase in CO release were observed above 60% SOC, as well as increases in hydrogen and short chain hydrocarbons such as ethylene and acetylene which lead to a decrease in the lower flammability limit from 15 vol% at 10% SOC to ~8 vol% at 40% SOC and above. Due to this decrease in lower flammability limit in released gases at higher SOC, fewer cells are required to create an explosive mixture in a given volume. Large-scale tests conducted by thermal abuse of over 500 18650 cells in an enclosure resulted in higher per Wh concentrations of hydrocarbons, hydrogen, carbon monoxide and carbon dioxide relative to single cells, which the authors attributed to higher maximum temperatures obtained in the large-scale tests.

Some of the hazards listed in this section may remain after a deactivation method has been applied. Batteries which are physically intact still contain any hazardous chemicals included in the electrolyte. A lithium-ion battery which has been discharged to 0V would be incapable of undergoing thermal runaway and robust toward abuse but would still contain flammable electrolyte which if ignited would contribute to a fire's intensity. End of life batteries which have been electrically isolated by activation of protective circuitry / fuses may present additional challenges, as the energy in these devices cannot be extracted through the electrical terminals used to store the energy. From this perspective, identifying effective evaluation criteria for deactivation methods is as important as developing the methods themselves.

3. DEACTIVATION METHODS

As described in the previous section, lowering the state of charge (SOC) of a lithium-ion battery is an effective route to avoid or limit energetic failures in response to abuse. Several reports on LIB recycling processes begin with a complete electrical discharge of the cells or batteries prior to some method of mechanical disassembly (23) (24). Harper et al. suggests that the recovered energy from discharging large battery packs and modules may help to offset the energy costs of subsequent recycling steps (25). Alternative methods to de-activate batteries prior to recycling include immersion in salt-water baths or "thermal" pre-treatment, sometimes described as pyrolysis, which subjects batteries to sufficiently high temperatures to both initiate thermal runaway and consume the flammable electrolyte. Even after discharging, batteries are typically shredded under inert or cryogenic conditions to avoid thermal runaway and fires. In some industrial settings, no deactivation step is utilized prior to shredding as mitigation methods such as an inert gas or water spray are considered sufficient (25). A review of available process information from the websites of prominent LIB recyclers Ascend Elements, Li-cycle, and Redwood materials indicates that all of these companies utilize mechanical shredding of batteries at the beginning of the recycling process (26) (27) (28). None of these companies mention discharging or any other form of deactivation. A technology overview video on the Li-cycle website states that "Lithium-ion batteries are safely processed in a water-based solution. This greatly improves safety, avoids potential hazards, such as fires, and starts the separation process." Instructions for shipping loose lithium-ion cells to Redwood Materials for recycling state, "Loose lithium-ion batteries: ship following DOT guidelines. Each battery should be placed in its own clear plastic bag (produce or sandwich bag) or tape the terminals with packing, electrical or duct tape."

Salt-water immersion is reported by several studies on battery recycling to be a preferred method for battery deactivation due to its flexibility, low cost, and relative safety, however corrosion of cell components and generation of secondary hazards including hydrogen gas and wastewater contaminated with battery electrolyte are known limitations (24) (29). Corrosion effects and discharge rates of 18650 LIB cells were reported by Shaw-Stewart et al. by evaluating 26 different saltwater solutions at a concentration of 5 wt% (30). The authors reported that while discharge rate was somewhat correlated with solution conductivity, corrosion effects played a critical role in removing energy from cells. Corrosion was found to be a function of solution pH and solute species, with mildly alkaline solutions of non-alkali salts showing the least amount of corrosion on the Ni-plated steel cell cans. Meanwhile, cells immersed in NaCl solutions while having a near neutral pH and high conductivity were heavily corroded within hours of exposure to the solution preventing voltage readings after a few hours. Yao et al. measured the composition of supernatants following LIB immersion in saltwater solutions using NaCl, $FeSO_4$ and $MnSO_4$ and observed high concentrations of electrolyte and electrode species (phosphorous, lithium,

cobalt) in the NaCl solutions (31). These corrosion effects have also been reported to impact the abuse response of lithium-ion batteries. Tao et al. reported that for 2.6 Ah 18650 cells immersed in 3.5 wt% NaCl solutions for varying times, cells underwent thermal runaway after 12 hours in solution when starting at 100% SOC when subjected to an open flame, and experienced higher heat release rates when immersed for 2-6 hours (32). The authors attributed the increase in heat release rate to corrosion of the 18650 header, which they speculate interfered with proper venting of the cell in response to external heating. A follow-on study by the same group exposed small packs of 18650 to 3.5 wt% NaCl solutions and reached similar conclusions, finding that thermal runaway was still observed for pack exposed to an open flame after up to 12 hours in the saltwater solution (33).

One alternative deactivation method of note comes from startup company OnTo Technologies of Bend, Oregon, which uses a pressurized reactor to force carbon dioxide into sealed LIB. The CO_2 serves to both extract the flammable liquid electrolyte for collection and storage as well as chemically react with Li and lithiated carbon to form less reactive lithium carbonate (34). Through funding from the Department of Energy Lithium-ion Battery Recycling Prize and the Defense Logistics Agency, OnTo Technologies has demonstrated that small cells subjected to the CO_2 deactivation method contain no stranded Li and do not undergo thermal runaway in response to external heating or mechanical abuse. Limited information is available on the efficacy of OnTo Technologies' approach to larger batteries or various cell constructions.

A comparison of deactivation methods identified in the literature (saltwater immersion, electrical discharge, and shredding) are provided in Table 1.

Table 1 Comparison of deactivation methods

Method	Flexibility	Deployability	Affordability	Safety	Limitations
Saltwater immersion	High	High	High	Moderate	Corrosion, generation of H_2
Electrical Discharge	Moderate	Moderate	Low to Moderate	High	Many require dynamic load bank / manual interaction with energized terminals
Shredding	Moderate	Low	Low	Low to Moderate	Requires preceding deactivation step or inert / cryogenic conditions

Pyrolysis or thermal treatment of batteries shares virtually the same advantages and disadvantages as shredding and is therefore not included in Table 1. Carbon dioxide electrolyte extraction was also excluded due to being unique to OnTo Technology, which limited the available information for comparison to other deactivation methods. Comparison factors are defined below:

1. **Flexibility:** Deactivation method should accommodate a wide variety of cell and battery designs, chemistries, and form factors
2. **Deployability:** Deactivation method should be easily accomplished whenever needed without specialized equipment or facilities.
3. **Affordability:** Deactivation method should have a reasonable cost such as not to prohibit subsequent desirable processes including battery recycling.
4. **Safety:** Deactivation method should not introduce or exacerbate hazards to people or the environment.

While the comparisons provided in Table 1 are intended to be qualitative, some explanation of each category is as follows:

Saltwater immersion can proceed with any energized cell type. However, at very high voltages, additional hazards may be generated. No special equipment is required beyond good ventilation and a water-tight, non-reactive container. Many demonstrations have utilized NaCl, which is low cost and commonly available. Less corrosive salts have been reported which may impact affordability. The main

hazards associated with deactivation by saltwater immersion are the generation of hydrogen gas, which is flammable at very low concentrations, and the possibility of generating wastewater contaminated with battery electrolyte.

Electrical discharge is highly effective and generates no hazardous waste streams when properly implemented. Critically, an electrical load must be sized appropriate to the device being deactivated, which reduces the method's flexibility and potentially increase cost substantially. Depending on the sophistication of the discharge method, the deployability may be acceptable for many applications. However, large dynamic load banks may not be easily transportable or have a high cost, making centralized deactivation more economical.

Shredding of end-of-life batteries is common practice in the recycling industry. However, batteries must be separated according to chemistry (e.g. a lead-acid shredding process cannot accept lithium-ion cells) both for safety and process efficiency reasons. Some reports indicate that only certain LIB are cost effective to recycle, notably those containing a larger component of Ni and Co; inclusion of other types such as lithium iron phosphate (LFP) would reduce the profitability of the recycling process. Shredding of energetic batteries requires specialized, expensive facilities intended to mitigate or contain battery fires, which significantly reduces both the deployability and affordability of shredding as a deactivation method. In an appropriately designed facility, the safety of battery shredding may be sufficiently safe. However, like any industrial process involving heavy equipment and toxic chemicals, well trained personnel would be required.

From the comparison of deactivation methods in Table 1, saltwater immersion was identified as a promising candidate

4. EXPERIMENTAL EVALUATION OF SALTWATER IMMERSION

An experimental evaluation of deactivation by saltwater immersion was conducted at the U.S. Naval Research Laboratory. Three experimental thrust areas were pursued, 1) evaluation of electrolysis currents in saltwater solutions using ideal, non-corrodible (platinum) electrodes, 2) evaluation of corrosion of electrode metals commonly used in battery cells in saltwater solutions, and 3) evaluation of lithium-ion cells immersed in saltwater as a deactivation method. Salt selection was narrowed to three materials – ammonium dihydrogen phosphate ($(NH_4)H_2PO_4$), ammonium bicarbonate ($(NH_4)HCO_3$), and sodium chloride (NaCl) as a control. All three salts are low cost, relatively non-toxic (ammonium bicarbonate is considered an irritant), and readily soluble in water. Critically, Shaw-Stewart et al. reported that $(NH_4)H_2PO_4$ and $(NH_4)HCO_3$ were two of the least corrosive solutes during saltwater immersion of 18650 form lithium-ion cells out of 26 salts surveyed (30). The conductivity and pH of saltwater solutions was measured using a Horiba LAQUAact PC-110 portable meter. For all the salts selected, solution conductivity is directly related to concentration. Solution pH is also influenced by the salt species used but was not found to be sensitive to solution concentration within the range of concentrations evaluated. A plot of solution conductivities and pH at various concentrations and molarities are shown in Figure 1 and Figure 2, respectively. Note that for a 20 wt% / 3.42 M NaCl solution, the maximum conductivity range of the meter (200 mS/cm) was exceeded, therefore a value of 200 mS/cm was recorded for this solution. From the conductivity plot in Figure 1, concentrations with identical conductivity were identified. A concentration of 3.5 wt% NaCl, which is the nominal concentration of seawater, has a conductivity of 54 mS/cm. A conductivity of 54 mS/cm was also identified for solutions of 11 wt% $(NH_4)H_2PO_4$ and 5.8 wt% $(NH_4)HCO_3$. These iso-conductivity solutions concentrations were used in several electrolysis and cell immersion experiments to isolate the effects of the salt species rather than the solution concentration.

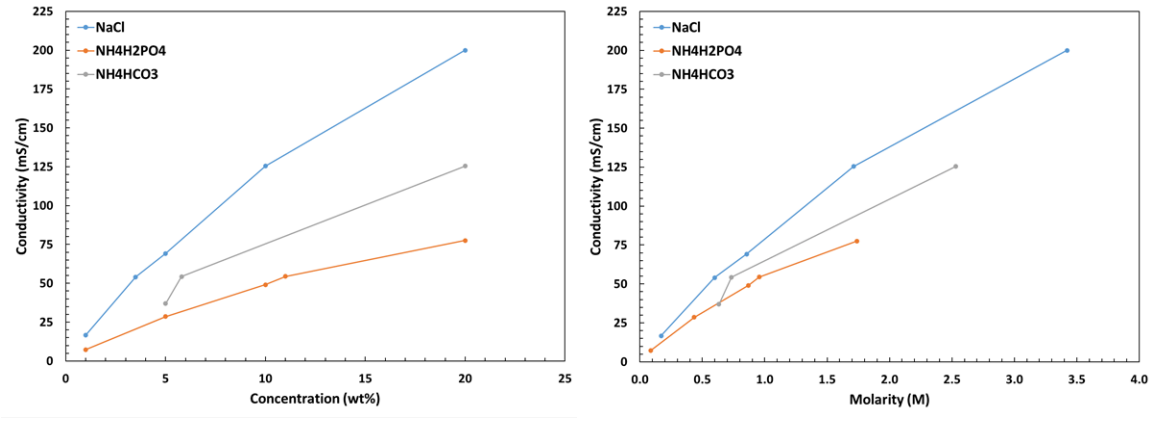

Figure 1 Saltwater solution conductivity as a function of concentration (left) and molarity (right).

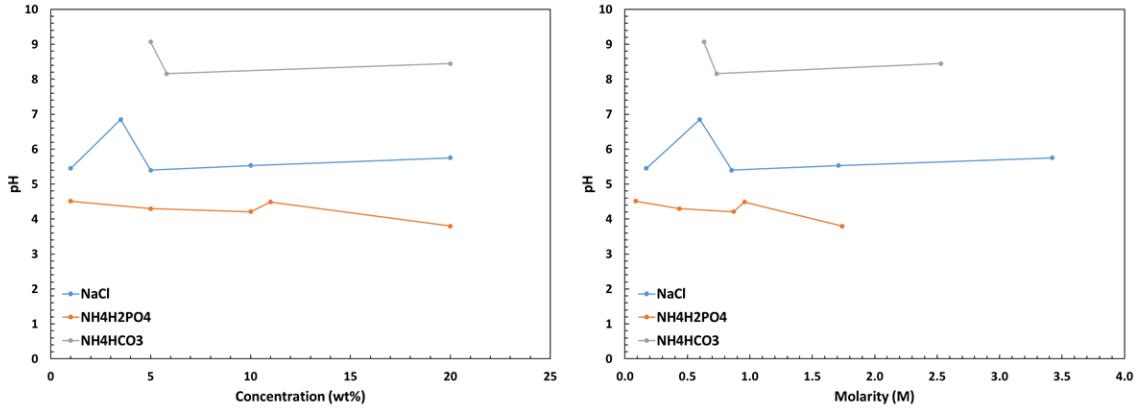

Figure 2 Saltwater solution pH as a function of concentration (left) and molarity (right).

The impact of solution temperature on conductivity was also investigated for $(NH_4)H_2PO_4$ solutions and found to have no effect as shown in Figure 3. Similar trends are expected for all salts provided the concentration evaluated is suitably far from the solubility limit, which is also influenced by solution temperature.

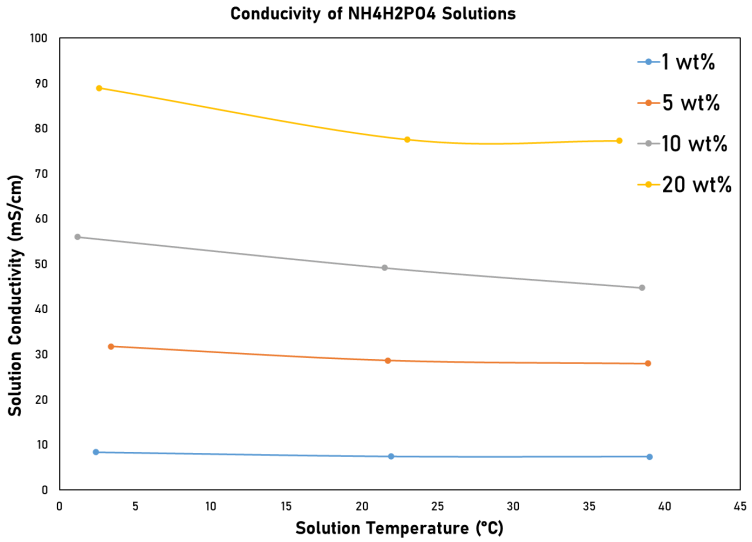

Figure 3 Solution conductivity vs. solution temperature for $(NH_4)H_2PO_4$ solutions.

4.1 ELECTROLYSIS OF SALTWATER SOLUTIONS

Three-electrode measurements were used to evaluate the electrolysis current produced in various saltwater solutions as a function of solution concentration and temperature. The three-electrode test cell utilized a 0.75 mm diameter, 3 mm long platinum wire as working electrode, platinum mesh as counter electrode, and an Ag/AgCl reference electrode. Platinum was selected as the working and counter electrode material to avoid consumption of the electrodes due to electrolytic corrosion, while the counter electrode was sized to have significantly greater area than the working electrode. By using the platinum working electrode, the only reactions available were the electrochemical decomposition of the salt or solvent (e.g. H_2O molecules). In this way, the electrolysis current for a given solution can be evaluated as a function of voltage. For a given solution and applied potential, a higher electrolysis current should translate to a faster rate of deactivation, therefore maximizing electrolysis current is desirable. Glassy carbon was initially evaluated as a less catalytically active alternative to platinum, however vigorous gas evolution during electrolysis was observed to exfoliate the glassy carbon electrode. The Ag/AgCl reference electrode provides a fixed electrochemical potential and experiences no current flow during the electrolysis experiments. A schematic and photograph of the three-electrode cell is shown in Figure 4. A fine stream of bubbles is generated from the working electrode during electrolysis experiments, which can block the surface of the electrode. These bubbles were removed using magnetic stirring during the electrolysis experiments, which removes the bubbles as seen in Figure 4.

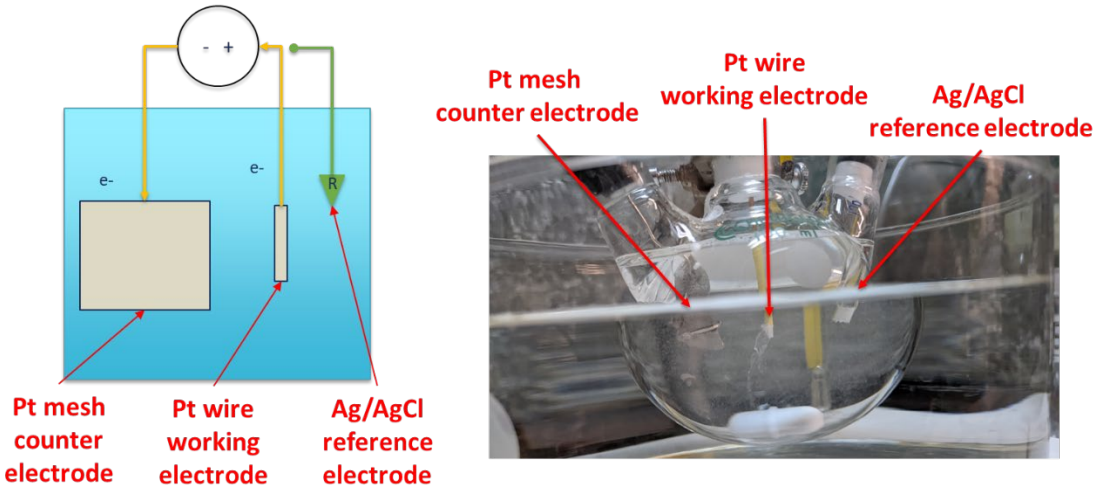

Figure 4 Schematic (left) and photograph (right) of three-electrode electrochemical cell.

Iso-conductivity solutions of NaCl, $(NH_4)H_2PO_4$, and $(NH_4)HCO_3$ were evaluated by cyclic voltammogram (CV) at a scan rate of 10 mV/s using a potential range of +3V to -3V vs open circuit. A

current vs. voltage (I vs. V) plot from the CV experiment is shown in Figure 5. As shown in Figure 5, all three solutions show roughly equivalent behaviors as a function of voltage, with the onset of oxidizing currents occurring at roughly +1.0 V to +1.5 V vs. Ag/AgCl, and onset of reducing currents occurring at roughly -1.0 V to -1.5 V vs. Ag/Cl. Beyond the onset potentials and up to the maximum potentials of approximately +3 V and -3 V vs. Ag/AgCl, vigorous bubbling at the working electrodes was observed in all solutions, confirming the production of a gaseous product.

Water electrolysis is assumed to be the main source of the observed current, with anodic (oxidizing, and in this case positive) potentials attributed to oxygen evolution and cathodic (reducing, and in this case negative) potentials are attributed to hydrogen evolution. Under ideal conditions, slight shifts in the onset potential of current flow can be attributed to solution pH, with low (acidic) pH shifting the onset of both water oxidation and water reduction to higher (i.e. more positive) potentials. However, this would predict the mildly acidic $(NH_4)H_2PO_4$ solution (pH ~ 4.5) would have highest onset potentials, followed by neutral NaCl (pH ~ 6.9), and mildly basic $(NH_4)HCO_3$ (pH ~8.2). Instead, the onset of oxidative current is seen first in the NaCl solution, with $(NH_4)H_2PO_4$ and $(NH_4)HCO_3$ showing oxidative current at almost identical potentials. An additional feature (a small peak) is observed in the NaCl solution centered at 1.4 V vs. Ag/AgCl which is plausibly attributed to the evolution of chlorine gas, which may explain the unexpected ordering of anodic onset potentials. Similarly, trends in reducing potentials are not cleanly predicted by pH alone. The lowest pH solution $(NH_4)H_2PO_4$ does reduce first as expected, however the highest pH $(NH_4)HCO_3$ solution begins reducing before the neutral NaCl solution. Again, an additional feature in the I vs. V plot may explain this behavior, as a small peak centered at -1 V vs. Ag/AgCl is observed for the $(NH_4)HCO_3$ solution, which is possibly the reduction of the bicarbonate (HCO_3^-) anion.

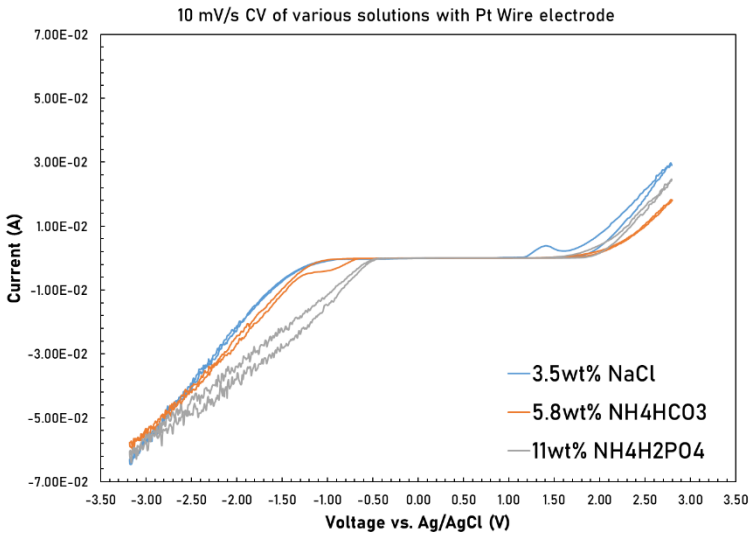

Figure 5 Current vs. Voltage (I vs. V) plot produced by a cyclic voltammogram of 3.5 wt% NaCl, 5.8 wt% $(NH_4)HCO_3$, and 11 wt% $(NH_4)H_2PO_4$ saltwater solutions using three-electrode test cell.

Electrolysis experiments of $(NH_4)H_2PO_4$ solutions with concentration ranging from 5-20 wt%, corresponding to 29 mS/cm to 78 mS/cm solution conductivity, were evaluated using the 3-electrode electrochemical cell. Current vs. Voltage plots for the $(NH_4)H_2PO_4$ solutions is shown in Figure 6, which shows no changes in onset potential. Interestingly, the cathodic current shows a stronger dependence on solution conductivity than the anodic current. In an acidic solution, the cathodic electrolysis reaction is assumed to be

$$2H^+ + 2e^- \rightarrow H_2,$$

while the anodic electrolysis reaction is assumed to be

$$H_2O \rightarrow O_2 + 4H^+ + 4e^-.$$

Oxygen evolution is generally understood to have more sluggish electrochemical kinetics than hydrogen evolution, which may provide some explanation as to why the positive anodic potentials do not show a strong dependence on salt concentration (35).

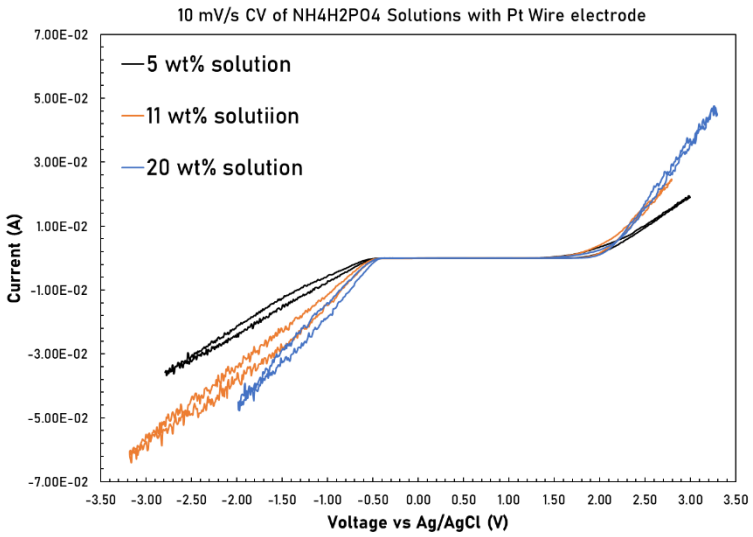

Figure 6 Current vs. Voltage (I vs. V) plot produced by a cyclic voltammogram of 5 wt%, 11 wt%, and 20 wt% $(NH_4)H_2PO_4$ solutions using three-electrode test cell.

While three electrode measurements provide a reference potential to compare against the working electrode, electrochemical devices only have two electrodes. Therefore, two electrode electrolysis measurements were also evaluated. Platinum electrodes were used with an identical experimental setup to that shown in Figure 4. A constant potential of +4 V was applied in the two-electrode electrolysis cell, representing a typical open-circuit potential for a full charged lithium-ion cell. A relatively stable current was observed for 300 seconds in response to a +4 V potential as shown in Figure 7, with the highest current observed in a 40 wt% solution heated to 60 °C. Average currents for the +4 V two-electrode electrolysis experiments at room temperature (~23 °C) and 40 °C are presented in Figure 8, which generally show an increase in current with solution concentration. Solution temperature is seen to influence electrolysis current more as solution concentration increase, likely due to the solubility limit of $(NH_4)H_2PO_4$. As seen in Figure 7 and Figure 8, the electrolysis current at room temperature in 40 wt% $(NH_4)H_2PO_4$ was actually slightly below the value for 20 wt% $(NH_4)H_2PO_4$, which is not observed at 40 °C. The nominal solubility limit of $(NH_4)H_2PO_4$ is 40 wt% at room temperature, and the 40 wt% solution was observed to have a cloudy appearance at room temperature.

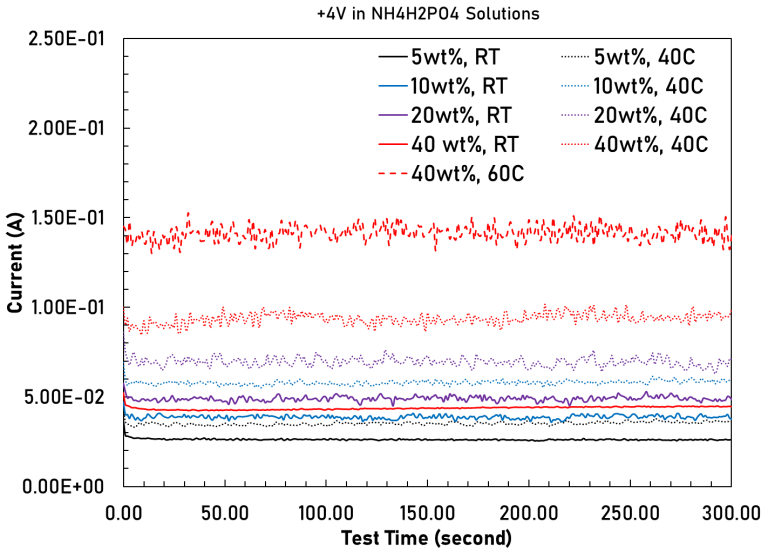

Figure 7 Current vs. time response for $(NH_4)H_2PO_4$ solutions subjected to +4V in a two-electrode test cell.

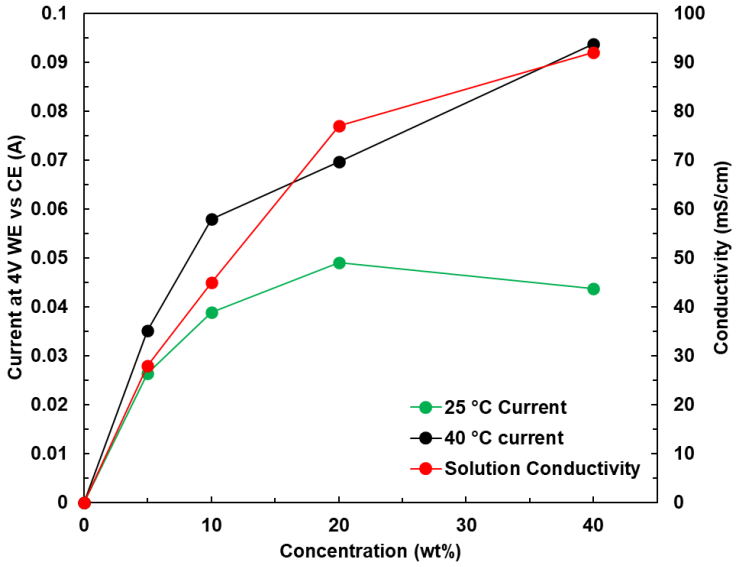

Figure 8 Average current for +4V two-electrode electrolysis of $(NH_4)H_2PO_4$ solutions.

4.2 CORROSION OF COMMON CELL MATERIALS IN SALTWATER

Four metals were selected to evaluate corrosion behavior during electrolysis – aluminum, copper, nickel, and a mild steel (1010 carbon steel). These metals are intended to represent common electrode / terminal electrical contacts found in a variety of electrochemical cell types. A two-electrode configuration was used analogous to the experimental setup using platinum electrodes in the previous section, however while the previous section's experimental setup utilized a platinum mesh counter electrode such that only the working electrode area would limit the reaction rate, the corrosion measurements utilized an identical electrode area for both working and counter electrode. Electrodes were sized to have identical area across material types and separated by a constant 20 mm independent of the saltwater solution used. Experiments conducted included a cyclic voltammogram analogous to the data presented in Figure 5 and Figure 6, as well as constant-potential measurements analogous to the data presented in Figure 7. Because the electrode materials were identical, only positive potentials relative to open circuit were considered, however it should be noted that the relative potential of the counter electrode would have been negative relative to a reference electrode like Ag/AgCl used in Figure 5 and Figure 6.

Cyclic voltammograms collected at a 10 mV/s scan rate for the four selected metals tested in the three iso-conductivity solutions described in the previous section are shown in Figure 9, Figure 10, Figure 11, and Figure 12. Each metal and solution combination shows a unique behavior, indicating that both the electrode material and salt species have a strong influence on electrolysis behavior. For the Current vs. Voltage response for the aluminum wire electrodes shown in Figure 9 shows that measurable current was only observed in the 3.5 wt% NaCl solution. This implies that one or both of the anodic or cathodic reactions, presumed to be oxygen evolution and hydrogen evolution, respectively, were unable to proceed when using an aluminum electrode. Further experimentation in which only the working electrode is aluminum is needed to determine which reaction prevents electrolysis from occurring in the 5.8 wt% $(NH_4)HCO_3$ and 11 wt% $(NH_4)H_2PO_4$ solutions.

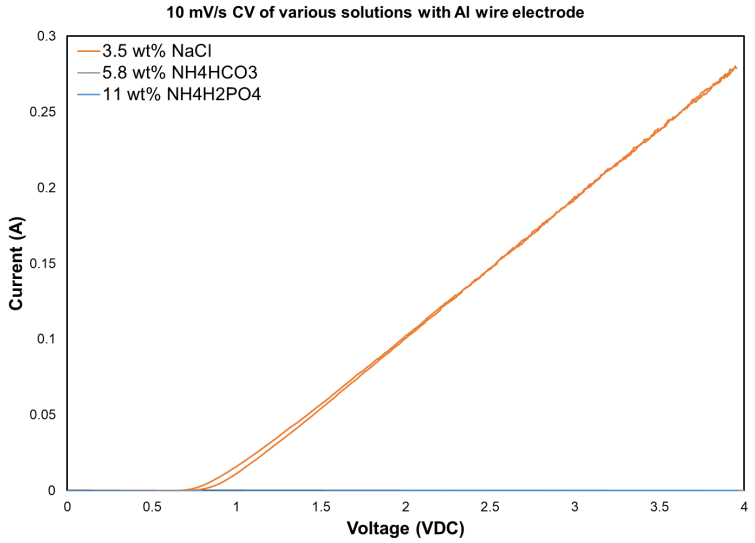

Figure 9 Current vs. Voltage (I vs. V) plot produced by a cyclic voltammogram of 5 wt%, 11 wt%, and 20 wt% $(NH_4)H_2PO_4$ solutions using two-electrode cell with aluminum electrodes.

Current vs. voltage plots produced using copper wire electrodes shown in Figure 10 resulted in some current flow for all solutions, however with notably different features in each solution. Only the 11 wt% $(NH_4)H_2PO_4$ solution resulted in the linearly increasing current with voltage analogous to that observed with a platinum electrodes in Figure 6, while the 3.5 wt% NaCl and 5.8 wt% $(NH_4)HCO_3$ solutions both show an initial increase in current followed by a decrease above some voltage. This behavior likely implies that some electrolysis reaction involving the electrode material itself begins, but is then suppressed either by passivation of one or both electrode, for example due to the formation of an electronically insulating layer, or by rapid consumption of the electrode into solution.

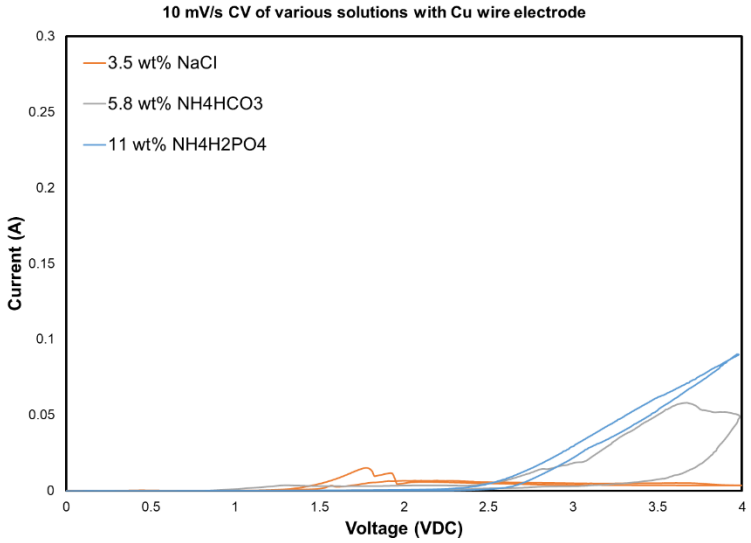

Figure 10 Current vs. Voltage (I vs. V) plot produced by a cyclic voltammogram of 5 wt%, 11 wt%, and 20 wt% $(NH_4)H_2PO_4$ solutions using two-electrode cell with copper electrodes.

Current vs. voltage plots collected with Ni electrodes shown in Figure 11 are the most reminiscent of those collected using platinum electrodes Figure 5 in, however the onset potential observed in 3.5 wt% NaCl solution is over 1.5 V lower than that observed in 5.8 wt% $(NH_4)HCO_3$ and 11 wt% $(NH_4)H_2PO_4$. While a small variation in onset potential is explainable by solution pH or the availability of competing electrolysis reactions occurring at lower potentials, the large potential difference observed is more likely related to the overpotential of water electrolysis in 5.8 wt% $(NH_4)HCO_3$ and 11 wt% $(NH_4)H_2PO_4$ relative to 3.5 wt% NaCl.

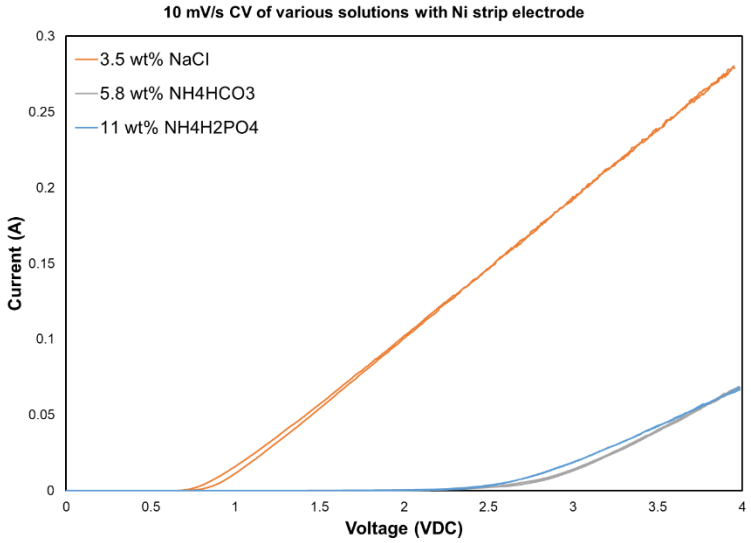

Figure 11 Current vs. Voltage (I vs. V) plot produced by a cyclic voltammogram of 5 wt%, 11 wt%, and 20 wt% $(NH_4)H_2PO_4$ solutions using two-electrode cell with nickel electrodes.

Current vs. voltage plots for mild steel electrodes are shown in Figure 12. The current response for 3.5 wt% NaCl and 5.8 wt% NH_4HCO_3 is observed to increase linearly after the onset potential, while the current response in 11 wt% $NH_4H_2PO_4$ first increases and then sharply decrease before increasing again. A similar current response was observed for Cu electrodes, and is again attributed formation of a passivating phase which is overcome at sufficiently high voltages.

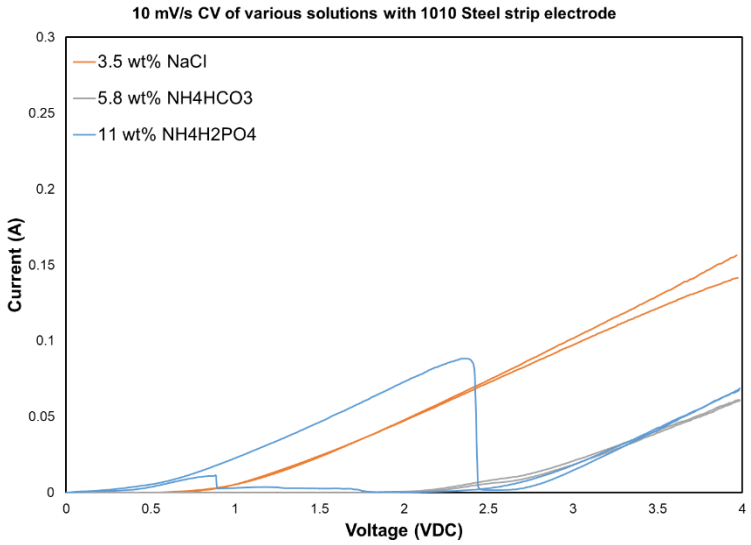

Figure 12 Current vs. Voltage (I vs. V) plot produced by a cyclic voltammogram of 5 wt%, 11 wt%, and 20 wt% $(NH_4)H_2PO_4$ solutions using two-electrode cell with steel electrodes.

Current vs. time plots produced during +4V potentiostatic electrolysis experiments using aluminum, copper, nickel, and 1010 steel electrodes are presented in Figure 13, Figure 14, Figure 15 for each of the iso-conductivity saltwater solutions. Currents observed in an 11 wt% $(NH_4)HPO_4$ solution shown in Figure 13 show that while copper electrodes initially produce the highest current, the current value drops to near zero after 2 hours of test time. A similar current declining behavior is observed for the nickel electrode after 5 hours, while current for the 1010 steel electrodes is stable for the entire 10-hour test duration. No current is observed using aluminum electrodes, which is consistent with the CV response shown in Figure 9.

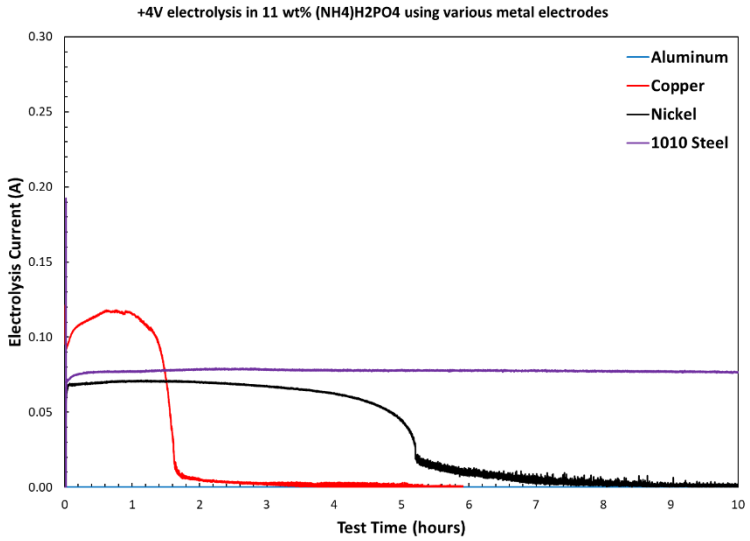

Figure 13 Current (A) vs. test time (hours) plot produced during potentiostatic electrolysis experiment in 11 wt%$(NH_4)H_2PO_4$ solutions.

Current response produced in 5.8 wt% $(NH_4)HCO_3$ solutions shown in Figure 14 are relatively stable for the entire 10-hour test duration. Similarly to the 11 wt% $(NH_4)HPO_4$ solution, no current is measured using aluminum electrodes.

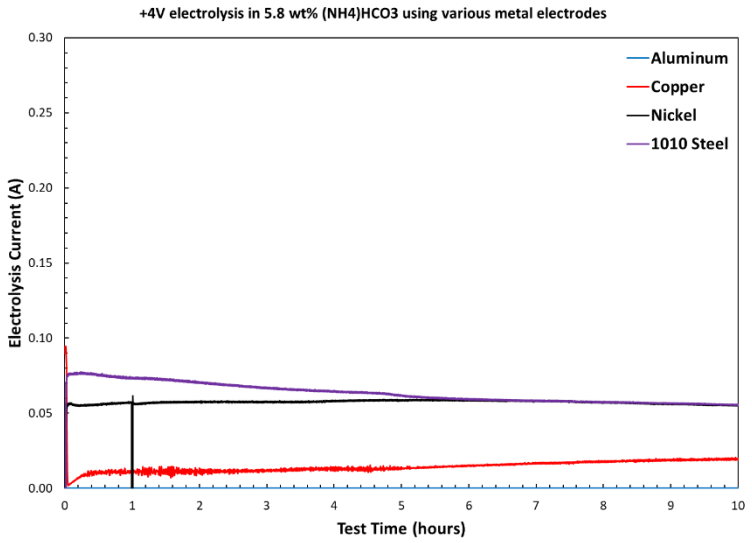

Figure 14 Current (A) vs. test time (hours) plot produced during potentiostatic electrolysis experiment in 5.8 wt% $(NH_4)HCO_3$ solutions.

Current responses for each electrode in 3.5 wt% NaCl shown in Figure 15 using aluminum, nickel, and steel electrodes is higher than for the other solutions evaluated, however a rapid current drop off is observed within one hour of test time. Only copper electrodes show a small, sustained current for most of the test duration.

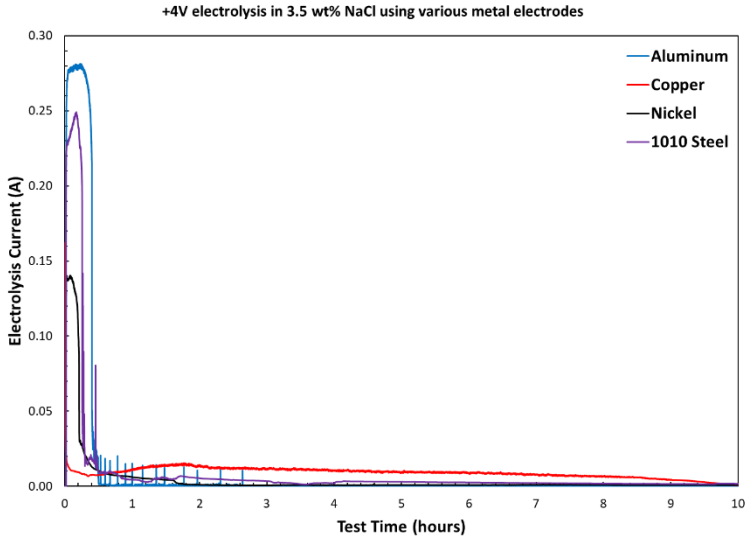

Figure 15 Current (A) vs. test time (hours) plot produced during potentiostatic electrolysis experiment in 3.5 wt% NaCl solutions.

The rapid drop-off in current observed during potentiostatic measurements in 11 wt% $(NH_4)H_2PO_4$ and 3.5 wt% NaCl solutions is clearly correlated with a loss in positive electrode mass. Mass

change of the positive electrode expressed as a % of the starting mass is presented for electrolysis experiments conducted at +2V, +3V, and +4V in the three iso-conductivity saltwater solutions as shown in Figure 16, Figure 17, and Figure 18. For electrodes which experienced a current decrease to near 0 amps during the +4V potentiostatic electrolysis experiments (e.g. Cu and Ni electrodes in 11 wt% $(NH_4)H_2PO_4$ and all metals in 3.5 wt% NaCl), the positive electrode mass change is near -100%, indicating the positive electrode was completely consumed during the electrolysis experiment. While the positive electrode is expected to undergo the anodic electrolysis reaction (oxygen evolution), other anodic reactions include the oxidation of the metal electrode into metal cations, which can then be dissolved into the saltwater solution. Positive electrode mass change also shows some correlation with potentiostatic voltage, with higher voltages corresponding to both higher currents and a greater mass loss.

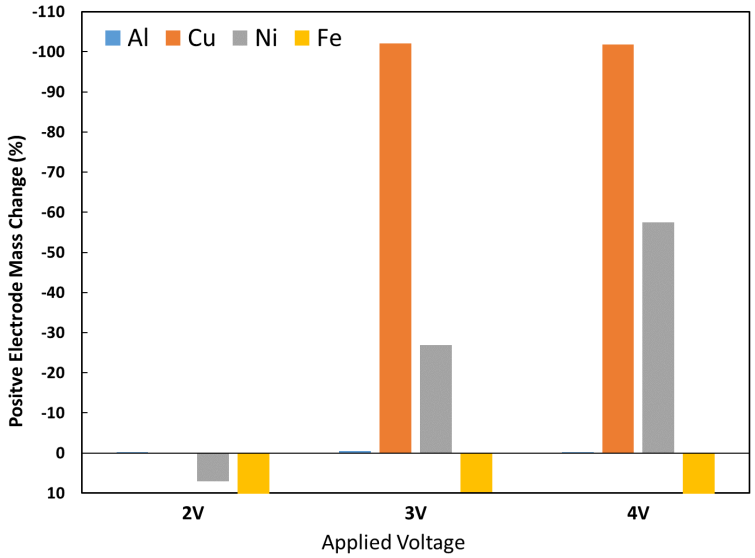

Figure 16 Positive electrode mass loss during a 10-hour electrolysis experiment as a function of applied potential and electrode material in 11 wt%$(NH_4)H_2PO_4$ solutions.

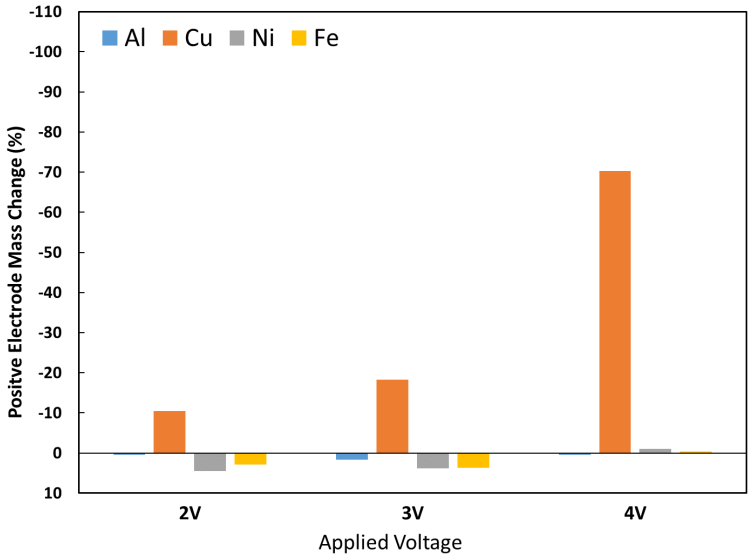

Figure 17 Positive electrode mass loss during a 10-hour electrolysis experiment as a function of applied potential and electrode material in 5.8 wt% $(NH_4)HCO_3$ solutions.

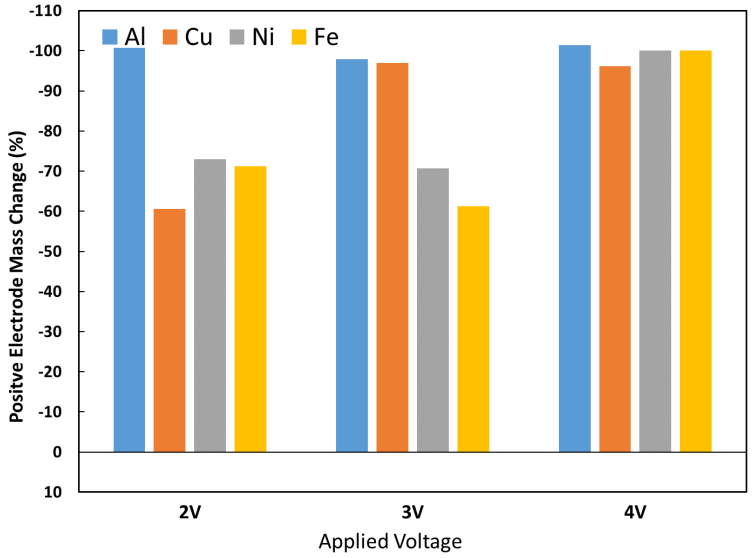

Figure 18 Positive electrode mass loss during a 10-hour electrolysis experiment as a function of applied potential and electrode material in 3.5 wt% NaCl solutions.

Consumption of the electrodes used during the electrolysis experiment had a strong influence on the total electrical energy, expressed as capacity in mAh, as shown in Figure 19, Figure 20, and Figure 21. While for 11 wt%$(NH_4)H_2PO_4$ and 5.8 wt% $(NH_4)HCO_3$ solutions, the capacity dissipated during the 10-hour electrolysis experiment increases with poteniostatic voltage, with the exception of the copper

electrodes in 11 wt%$(NH_4)H_2PO_4$ which were completely consumed at +3V and +4V as shown in Figure 16. Meanwhile, the total capacity dissipated in 3.5 wt% NaCl solutions appears to be invariant of the electrode material used or the applied potential, despite the higher currents observed relative to the other saltwater solutions seen in Figure 15. Consumption of the electrodes in 3.5 wt% NaCl limits the amount of capacity dissipated by electrolysis, which is clearly reflected in the high positive electrode mass losses in Figure 18.

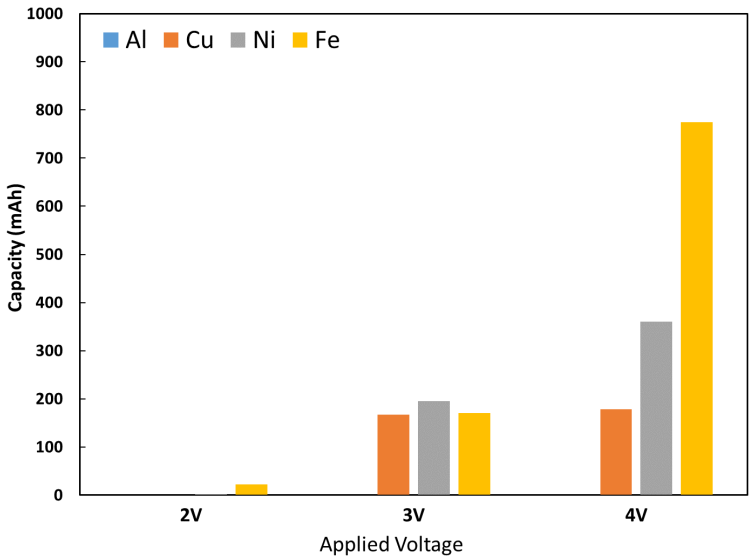

Figure 19 Energy dissipated during a 10-hour electrolysis experiment as a function of applied potential and electrode material in 11 wt% $(NH_4)H_2PO_4$ solutions.

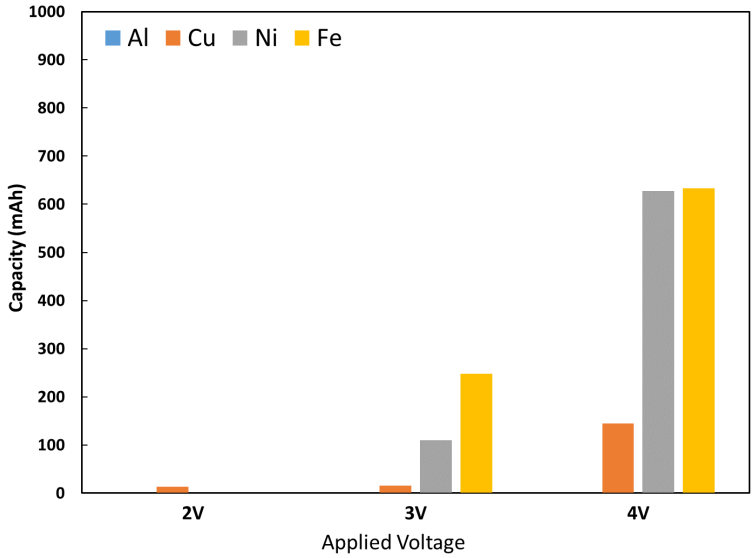

Figure 20 Energy dissipated during a 10-hour electrolysis experiment as a function of applied potential and electrode material in 5.8 wt% $(NH_3)HCO_3$.

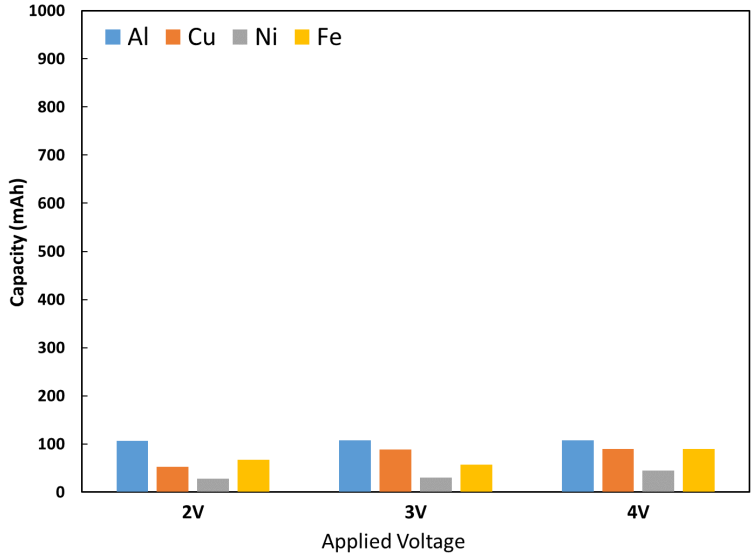

Figure 21 Energy dissipated during a 10-hour electrolysis experiment as a function of applied potential and electrode material in 3.5 wt% NaCl.

4.3 IMMERSION OF COMMERCIAL LITHIUM-ION CELLS IN SALTWATER

Saltwater immersion as a deactivation method was evaluated using commercial lithium-ion cells with an "18650" cylindrical form factor (18 mm diameter and 65 mm length). The cells utilized had a nominal capacity of 2.5 Ah between a voltage range of 2.5 V to 4.2 V and an outer can consisting of a Ni-plated mild steel. Within the hermetically sealed cell, a graphite anode is coated onto a copper current collector and a lithium-transition metal-oxide cathode is coated onto an aluminum current collector. Cells were charged to 100% state-of-charge and immersed in the three iso-conductivity saltwater solutions described in the previous sections for up to 96 hours (4 days). Continuous measurements of cell voltage were not possible during saltwater immersion experiments, as any conductor used to measure cell voltage would become energized and potentially consumed by the electrolysis process. Instead, cells were removed periodically from the immersion solution and the voltage was checked using a multimeter. Voltages for three identical cells immersed in iso-conductive saltwater solutions is shown in Figure 22. All the cells show a relatively steady decline in voltage for the first 24 hours, while after 72 hours the cell immersed in 3.5 wt% NaCl experiences a rapid voltage loss. After 96 hours, all cells have reached a voltage below the nominal 0% state of charge (2.5 V).

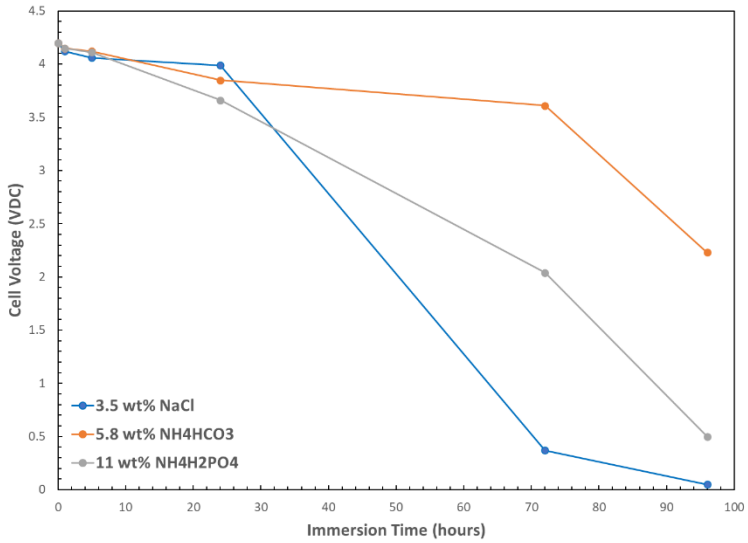

Figure 22 Voltages of 18650 lithium-ion cells immersed in iso-conductive saltwater solutions.

Photographs of the immersion solution, positive terminal, and negative terminal of the 18650 taken after 24 hours and after 96 hours in Figure 23 and Figure 24. At 24 hours, the 11 wt% $(NH_4)H_2PO_4$ solution is cloudy, while the positive terminal appears uncorroded and the negative terminal is covered in

brown deposits. These deposits can be mostly removed with gentle abrasing using laboratory tissue. After 96 hours, the 11 wt% $(NH_4)H_2PO_4$ solution is cloudy and both the negative terminal and positive terminal are coated in brown deposits. The 5.8 wt% $(NH_4)HCO_3$ solutions remain clear after both 24 and 96 hours, while some discoloration is observed on the positive terminal. Similar to the 11 wt% $(NH_4)H_2PO_4$ solution, the negative terminals of cells immersed in 5.8 wt% $(NH_4)HCO_3$ solutions are covered in brown deposits which can be removed with gentle abrasion. The positive terminal of cells immersed in 3.5 wt% NaCl have a markedly different appearance compared to the cells immersed in 11 wt% $(NH_4)H_2PO_4$ and 5.8 wt% $(NH_4)HCO_3$ solutions. Rather than observing discoloration, the positive terminal itself has been dissolved into the NaCl solution to reveal the underlying "burst disc". Likewise, NaCl solutions are significantly darkened by a large amount of brown and green precipitates. Interestingly, the negative terminals of cells immersed in 3.5 wt% NaCl solution seem unaffected. One explanation is that metal ions stripped by the anodic potential of the positive terminal in 11 wt% $(NH_4)H_2PO_4$ and 5.8 wt% $(NH_4)HCO_3$ solutions (e.g. Ni and Fe ions) remain in solution until they are reduced to form the deposits observed on the negative terminal. The same ions produced in 3.5 wt% NaCl may instead precipitate, which prevents deposition on the negative terminal but leads to the dark solution observed in Figure 23 and Figure 24.

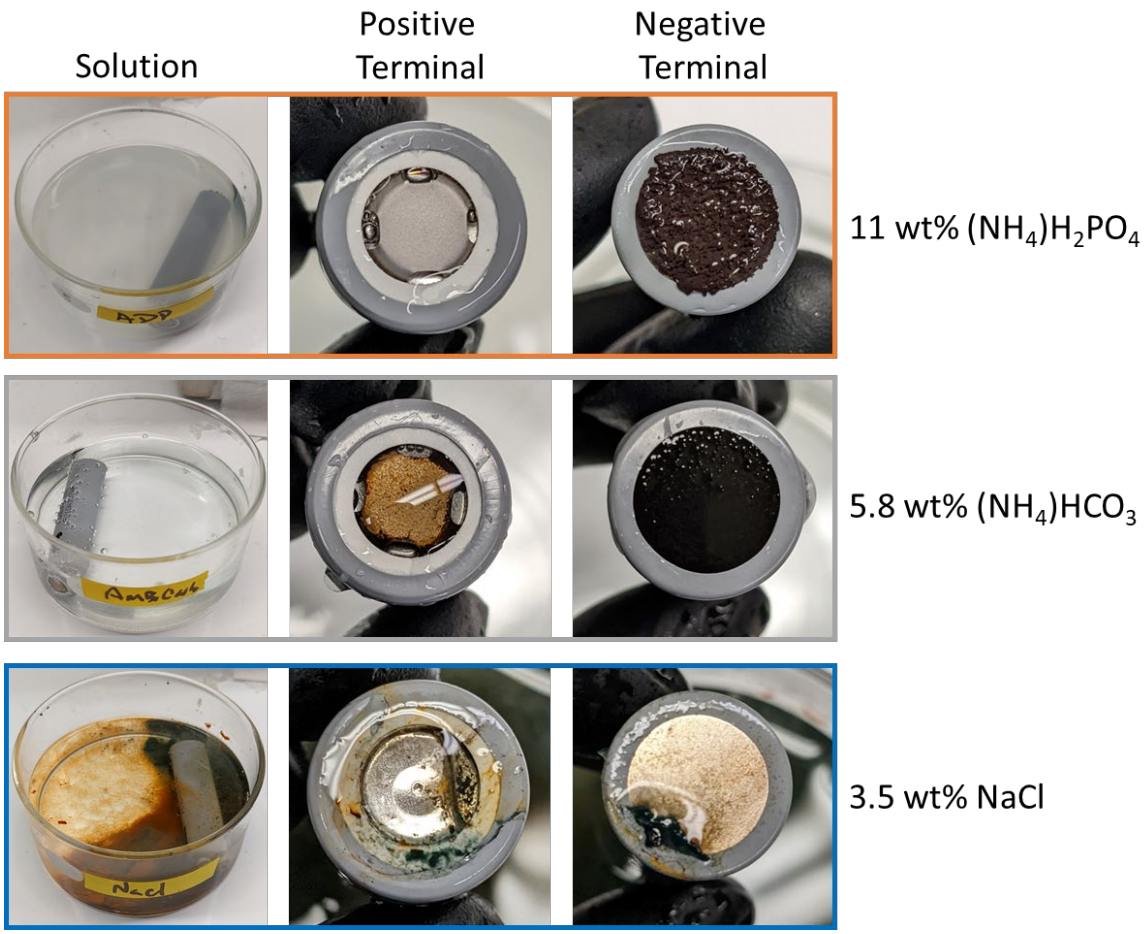

Figure 23 Photographs of saltwater solution, positive terminal, and negative terminal of 18650 lithium-ion cells after 24 hours of immersion.

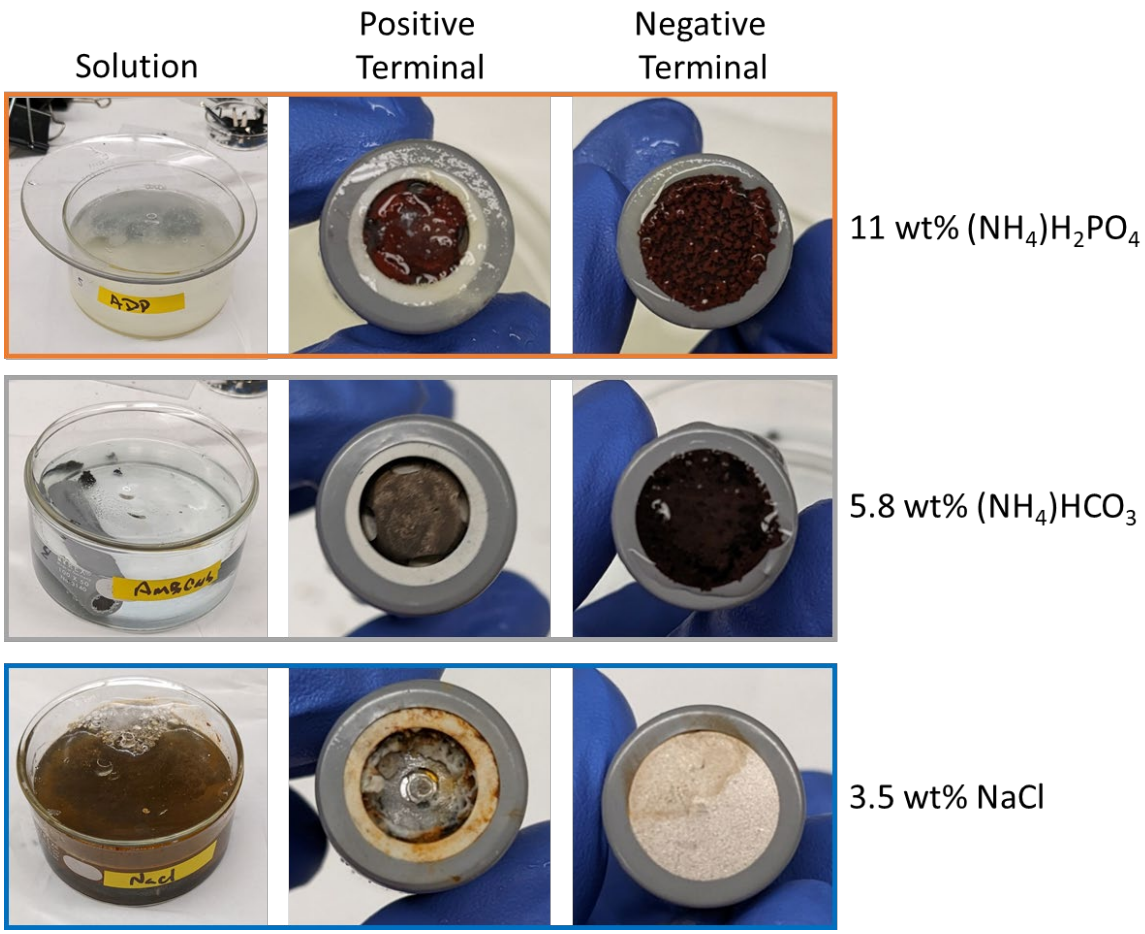

Figure 24 Photographs of saltwater solution, positive terminal, and negative terminal of 18650 lithium-ion cells after 96 hours of immersion.

Disassembly of the 18650 lithium-ion cells after saltwater immersion was conducted to determine whether the hermetically sealed cells had been breached due to corrosion of the cell casing. Cells which were electrically discharged to 0V were also disassembled for comparison. As shown in Figure 25, the anode (A) and cathode (C) electrodes recovered from electrically discharged cells and cells immersed in 11 wt% $(NH_4)HPO_4$ and 5.8 wt% $(NH_4)HCO_3$ appear similar and the active material coatings are mostly intact, while the electrodes extracted from the cell immersed in 3.5 wt% NaCl solution are severely degraded. This suggests that the positive terminal corrosion of cells immersed in 3.5 wt% NaCl breached the hermetic seal of the 18650 lithium-ion cell, allowing direct contact of the electrodes with the saltwater solution, as well as some electrolysis occurring from the electrodes themselves rather than the cell terminals, which is consistent with the mass loss observed for electrolysis experiments in 3.5 wt% NaCl solution (Figure 18). While this would lead to rapid loss in cell voltage, a breach of the cell also allows

for the electrolyte material to escape. In the case of lithium-ion batteries, the $LiPF_6$ salt can decompose on contact with water to form hydrofluoric acid (HF).

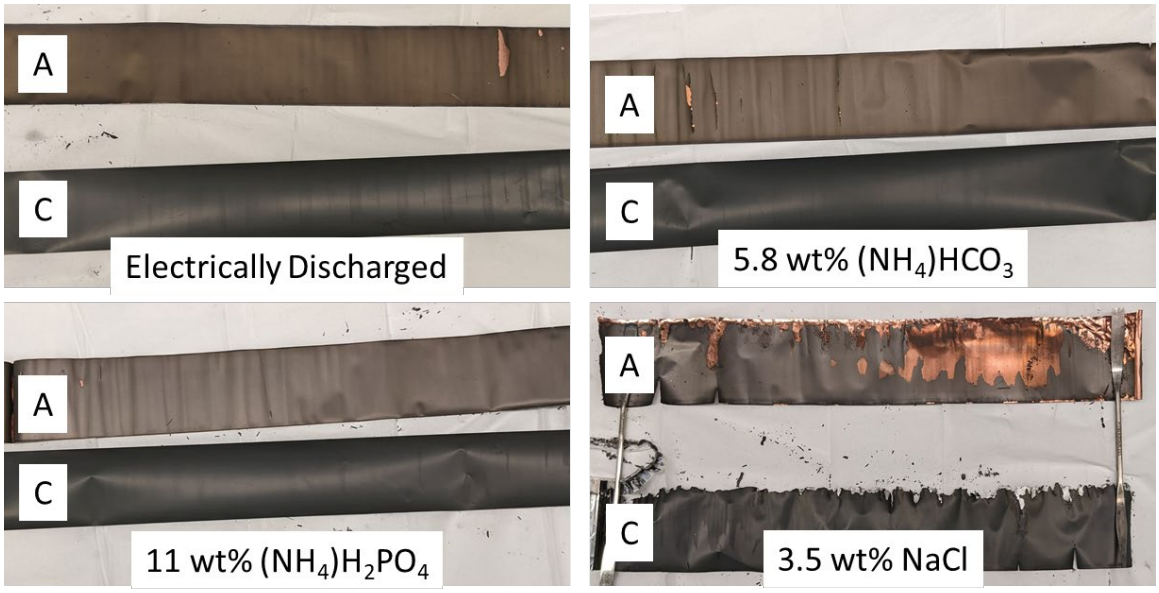

Figure 25 Photographs of 18650 lithium-ion cell anode (A) and cathode (C) after electrical discharge to 0V or 96 hours in saltwater solutions.

In order to verify that saltwater immersion had removed sufficient energy from the 18650 lithium-ion cells avoid energetic failures, cells immersed for 24 hours and 72 hours were subjected to external heating while inside of a pressure vessel. As shown in Figure 26, cells immersed for 24 hours in all iso-conductivity solutions undergo cell venting and thermal runaway, which is evidenced by sharp increases in temperature and pressure. A sharp drop in voltage attributed to activation of the current interrupt device (CID) by a build-up of pressure inside the 18650 cell header assembly also confirms that the cells are still hermetically sealed after 24 hours in saltwater solutions.

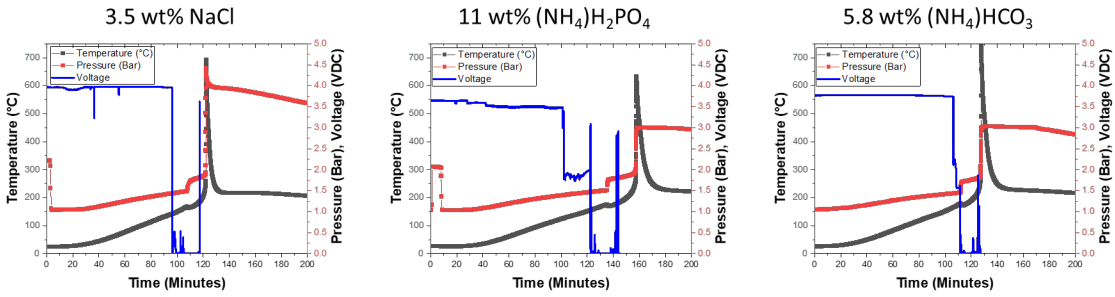

Figure 26 Voltage, pressure, and temperature response of 18650 lithium-ion cells subjected to external heating inside of a pressure vessel after 24 hours in saltwater solutions.

After 72 hours the 18650 cells immersed in 3.5 wt% NaCl no longer have a readable voltage and do not show any rapid increase in pressure or temperature in response to external heating (Figure 27). This observation is consistent with the appearance of the electrodes extracted from cells immersed in 3.5 wet% NaCl , which clearly indicate the cell casing had been breached (Figure 25). Meanwhile, cells immersed in 11 wt% $(NH_4)H_2PO_4$ and 5.8 wt% $(NH_4)HCO_3$ both show a clear voltage drop and pressure rise due to heating, with supports the conclusion that these cells are still sealed after 72 hours in these solutions. Only the cell immersed in 5.8 wt% $(NH_4)HCO_3$ experiences a rapid temperature rise indicating thermal runaway, which is consistent with the voltage plot presented in Figure 22, wherein only cells immersed in 5.8 wt% $(NH_4)HCO_3$ had a voltage above 0% state of charge (i.e. >2.5 V) after 72 hours.

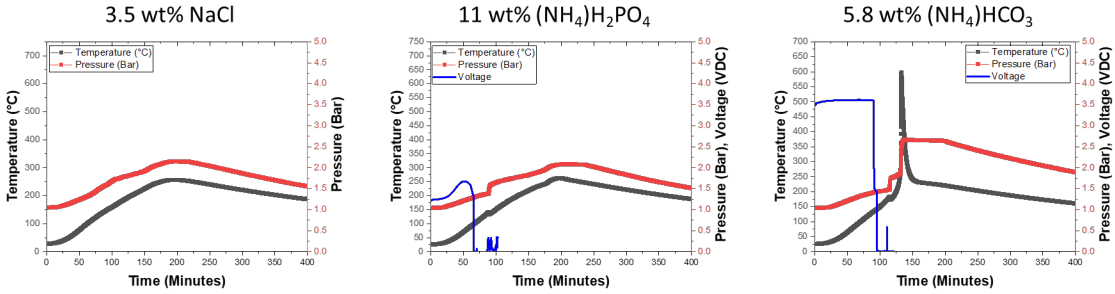

Figure 27 Voltage, pressure, and temperature response of 18650 lithium-ion cells subjected to external heating inside of a pressure vessel after 72 hours in saltwater solutions.

5. CONCLUSIONS AND RECOMMENDATIONS

Through a survey of available industrial and academic literature, saltwater immersion was identified as the most utilitarian method to deactivate end of life batteries. However, currently operating recycling facilities are believed to rely primarily on packing prior to transportation (e.g., taping off terminals and placing batteries in plastic bags) rather than any formal deactivation method. Batteries are then mechanically shredded in a controlled environment to dissipate residual energy and contain energetic failures. This method is effective but not deployable, and therefore does nothing to alleviate battery failures occurring during transportation.

An experimental evaluation confirmed that saltwater immersion of single lithium-ion cells can remove energy from these devices and preventing energetic failure in response to abuse, however the process is slow and generates additional hazards. Among the saltwater solutions identified, solutions of 11 wt% $(NH_4)\,H_2PO_4$ were the most effective at de-energizing cells while avoiding significant corrosion of the cell material, while solutions of 5.8 wt% $(NH_4)HCO_3$ were most effective at avoiding corrosion overall. Other salts are likely just as affective as the solutes studied in this report, as seen in section 4.2 corrosion behavior is dependent on both the salt species, the electrode material, and the applied potential. Solution concentration and temperature were shown to affect electrolysis current using platinum electrodes, and while increasing both would likely increase the rate of deactivation, this may also influence corrosion rates.

New methods are needed to deactivate batteries which optimize the parameters identified in Table 1, specifically that methods should be flexible, affordable, deployable, and safe. Cost is also a critical factor, though is likely dependent on scale as much as the particular method itself. Combining the benefits of saltwater immersion – low cost, chemistry and form-factor flexibility, and deployability with the high safety of controlled electrical discharge is one plausible path forward. Identifying quantitative criterion for evaluating deactivated batteries is also a critical need. Hypothetically, deactivated batteries may no longer need to be classified as hazardous waste, which would greatly reduce the cost of transporting these devices at the end of life.

6. REFERENCES

1. *Investigating the Role of Energy Density in Thermal Runaway of Lithium-ion Batteries with Accelerating Rate Calorimetry.* **Lamb, J, et al.** 060516, 2021, Journal of the Electrochemical Society, Vol. 168.
2. **National Transportation Safety Board.** *Safety Risks to Emergency Responders from Lithium-Ion Battery Fires in Electric Vehicles.* 2020. NTSB/SR-20/01.
3. **Samsung.** [Infographic] Galaxy Note7: What We Discovered. [Online] January 23, 2017. https://news.samsung.com/global/infographic-galaxy-note7-what-we-discovered.
4. **United States Envrionmental Protection Agency.** *An Analysis of Lithium-ion Battery Fires in Waste Management and Recycling.* 2021. EPA 530-R-21-002.
5. **Chauhan, Karn.** Apple Captures 7 Spots in 2021 List for Global Top 10 Smartphones. *Counterpoint.* [Online] March 8, 2022. https://www.counterpointresearch.com/global-top-10-smartphones-2021/.
6. **Energizer.** Energizer 522 Product Data Sheet. [Online] https://data.energizer.com/pdfs/522.pdf.
7. **Apple iPhone 12.** ***GSM ARENA.*** **[Online] https://www.gsmarena.com/apple_iphone_12-10509.php.**
8. Schuler, Mike. gCaptain. *'Potentially Catasrophic' – Container Loaded with Discarded Lithium Batteries Catches Fire Enroute to Port.* [Online] March 10, 2022. https://gcaptain.com/container-lithium-battery-fire/.
9. THE MARITIME EXECUTIVE. USCG Reports Another Fire in a Misdeclared Box of Scrapped Batteries. *The Maritime Executive.* [Online] March 14, 2022. https://maritime-executive.com/article/uscg-reports-another-fire-in-a-misdeclared-box-of-scrapped-batteries#:~:text=On%20August%2019%2C%202021%2C%20a,boxship%20for%20transport%20to%20China..
10. Electrochemical Safety Research Institute, Underwriters Laboratories Inc. *Safety in the Recycling of Lithium-ion Batteries.* 2022.
11. U.S. Energy Storage Association. *End-of-Life Management of Lithium-ion Energy Storage Systems.* 2020.
12. *A review of hazards associated with primary lithium and lithium-ion batteries.* Lisbona, D and Snee, T. 2011, Process Safety and Environmental Protection, Vol. 89, pp. 434-442.
13. *Experimental Analysis of Thermal Runaway in 18650 Cylindrical Li-ion Cells Using an Accelerating Rate Calorimeter.* Lei, B, et al. 14, 2017, Batteries, Vol. 3.
14. *A review of lithium-ion battery safety concerns: The issues, strategies, and testing standards.* Chen, Y, et al. 2021, Journal of Energy Chemistry, Vol. 59, pp. 83-99.
15. Roth, Peter E, et al. *Advanced Technology Development Program for Lithium-Ion Batteries: Thermal Abuse Performance of 18650 Li-Ion Cells.* Sandia National Laboratories. 2004. SAND2004-0584.
16. *Impact of State of Charge and Cell Arrangement of Thermal Runaway Propagation in Lithium Ion Battery Cell Arrays.* Lee, C, Said, AO and Stoliarov, SI. 8, 2019, Transportation Research Record, Vol. 2673, pp. 408-417.
17. *Safety of Lithium-ion Cells and Batteries withVarying States-of-Charge.* Joshi, T, et al. 14, 2020, Journal of the Electrochemical Society, Vol. 167.
18. *Transportation Safety of Lithium Iron Phosphate Batteries – A Feasibility Study of Storing at Very Low States of Charge.* Barai, A, et al. 5128, 2017, Scientific Reports, Vol. 7.
19. A. W. Golubkov, et al. Thermal runaway of commercial 18650 Li-ion batteries with LIF and NCA cathodes - impact of state of charge and overcharge. *RSC Advances.* 2015, Vol. 5.
20. *Review - Meta-review of Fire Safety of Lithium-ion Batteries: Industry Challenges and Research Contributions.* Diaz, LB, et al. 090559, 2020, Journal of the Electrochemical Society, Vol. 167.
21. *Toxix fluorid gas emissions from lithium-ion battery fires.* Larsson, F, et al. 10018, 2017, Scientific Reports, Vol. 7.

22. Maloney, T. ***Lithium Battery Thermal Runaway Vent Gas Analysis.*** **s.l. : Federal Aviation Administration, 2016. DOT/FAA/TC-15/59.**
23. ***Comprehensive Characterization of Shredded Lithium-ion Battery Recycling Material.*** **Peschel, C, et al. e202200485, 2022, Chemistry - A European Journal, Vol. 28.**
24. ***Recycling of Lithium-Ion Batteries—Current State of the Art, Circular Economy, and Next Generation Recycling.*** **Nuemann, J, et al. 2102917, 2022, Advanced Energy Materials.**
25. ***Recycling lithium-ion batteries from electric vehicles.*** **Harper, G, et al. 2019, Nature, Vol. 575, pp. 75-86.**
26. Ascend Elements. Innovation. [Online] December 2022. https://ascendelements.com/innovation/.
27. Li-cycle. Technology. [Online] December 2022. https://li-cycle.com/technology/.
28. Redwood Materials. Frequently Asked Questions. [Online] https://www.redwoodmaterials.com/recycle-with-us/#how-do-i-package-and-ship-batteries.
29. ***Pretreatment options for the recycling of spent lithium-ion batteries: A comprehensive review.*** **Yu, D, et al. 107218, 2021, Minerals Engineering, Vol. 173.**
30. ***Aqueous solution discharge of cylindrical lithium-ion cells.*** **Shaw-Stewart, J, et al. e00110, 2019, Sustainable Materials and Technologies, Vol. 22.**
31. ***An environmentally friendly discharge technology to pretreat spent lithium-ion batteries.*** **Yao, LP, et al. 118820, 2020, Journal of Cleaner Production, Vol. 245.**
32. ***An experimental investigation on the burning behaviors of lithium ion batteries after different immersion times.*** **Tao, C, et al. 118539, 2020, Journal of Cleaner Production, Vol. 242.**
33. ***The study of thermal runaway characteristics of multiple lithium batteries under different immersion times.*** **Tao, C, et al. 2022, Journal of Thermal Analysis and Calorimetry, Vol. 147, pp. 11457–11466.**
34. Sloop, SE. ***System and method for removing an electrolyte from an energy storage and/or conversion device using a supercritical fluid. 7,198,865*** **2007.**
35. ***Towards a generic understanding of oxygen evolution reaction kinetics in polymer electrolyte water electrolysis.*** **Schuler, T, et al. 2020, Enery & Environmental Science, Vol. 13, pp. 2153-2166.**